8-2009

X-ray Flow Visualization of a Circular Hydraulic Jump

Megan R. DiVall
Iowa State University

Theodore J. Heindel
Iowa State University, theindel@iastate.edu

Proceedings of the ASME 2009 Fluids Engineering Division Summer Meeting
FEDSM2009
August 2-6, 2009, Vail, Colorado USA

FEDSM2009-78035

X-ray Flow Visualization of a Circular Hydraulic Jump

Megan R. DiVall and Theodore J. Heindel*
Department of Mechanical Engineering
Iowa State University
Ames, Iowa 50011

ABSTRACT

The circular hydraulic jump is a product of the impingement of a vertical, circular jet upon a smooth horizontal surface. Previous studies of this phenomenon have used methods such as electrical contact probes, photography, and lasers to measure various features. This study utilizes X-ray computed tomography (CT) to visualize the circular hydraulic jump; analysis is then completed on the reconstructed 3D image. Time-averaged data of the film thickness before and after the jump and the jump radius, as measured from the X-ray CT images, compare well with available literature. Potential imaging improvements with the current equipment have been identified, particularly with respect to measuring film thickness.

INTRODUCTION

Hydraulic jumps occur when open liquid flow transitions from supercritical flow to subcritical flow. When the flow switches from supercritical to subcritical speeds, the liquid depth rises substantially over a short distance and creates an obvious "jump" in height. While certain types of hydraulic jumps can happen in places such as open channels and rivers, the focus of this study is on free jets impinging on flat surfaces, similar to what is found when water from your faucet hits the bottom of your kitchen sink. A hydraulic jump resulting from a vertical liquid jet impinging on a smooth horizontal surface is called a circular hydraulic jump. Flow inside the circular jump is very thin and flows supercritically until it reaches the jump, where it abruptly increases in height to dissipate kinetic energy and slow to a subcritical rate. This circle encompassing the jump region remains stationary and the radius of this circle is influenced by several factors, including the flow rate, the liquid viscosity, and the smoothness and shape of the surface over which it travels.

The circular hydraulic jump radius has been studied using many different data acquisition methods. One of the most common devices for this type of investigation is electrical contact probes [1-4]. The generally stationary and stable nature of a circular hydraulic jump also allows for photographic visualization, which was used by Rao and Arakeri [3] and Kate et al. [5]. Craik et al. [6] utilized a laser and dyed water to measure water film thickness. However, these methods do have disadvantages. For example, the electrical contact probe is by its nature invasive, and the laser and photographic methods require optical access and transparent fluids.

This paper reports preliminary data using an entirely different method of measurement to study the circular hydraulic jump: X-ray computed tomography (CT). This was accomplished using the unique X-ray Flow Visualization Facility at Iowa State University. The facility uses an X-ray source and detector/camera combination mounted opposite each other on a turn-table to record multiple time-averaged X-ray projections of the flow. The resulting data are then reconstructed using a multislice filtered back projection algorithm into a three-dimensional image that can be analyzed by "slicing" through the image to view any desired region of interest, all while being entirely noninvasive [7].

EXPERIMENTAL PROCEDURES

The free jet impingement system used in this study is schematically represented in Figure 1. The nozzle had an outer diameter of 6.3 mm and an inner diameter (identified as "d" in Figure 1) of 4.8 mm. The separation distance between the nozzle exit and the plate surface was H ≈ 4.2 cm (the exact value depends on how tight the cover is attached). Several

* Corresponding Author: T.J. Heindel, theindel@iastate.edu

studies, including Rao and Arakeri [3] and Ellegaard et al. [1], have noted that nozzle separation distance had a negligible impact on the formation of the hydraulic jump, so the separation distance was fixed for this study. The jet impinged upon a smooth horizontal acrylic disk which was 6.7 cm thick and 23 cm in diameter. The disk edges where sanded to allow the liquid to flow freely from the plate surface [3]. The nozzle and disk were housed in a high-density polyethylene bucket fitted with a drain allowing a return feed to the pump. Deionized water was circulated through the system by a closed-loop pump whose operation was regulated by a variable-voltage DC motor controller. The system was calibrated beforehand via the "catch and weigh" method to find the relationship between flow rate and motor controller setting.

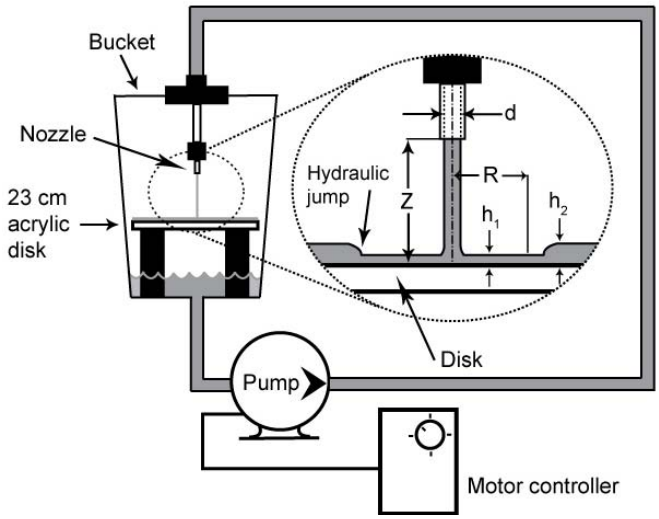

FIGURE 1: SCHEMATIC LAYOUT OF THE EXPERIMENTAL SETUP WITH CLOSE-UP OF THE REGION OF INTEREST.

Details of the X-ray flow visualization facility used in this study are found elsewhere [7] and only a summary is provided here. The X-ray imaging system consists of two X-ray sources and image detectors, offset 180° from each other. The X-ray sources and detectors are mounted on a slewing ring (a donut-shaped gear) with a 1 m ID which allows complete rotation around the flow of interest. For computed tomography (CT) imaging, a single source and detector are used. The detector is a 44×44 cm cesium-iodide phosphor screen coupled to an Apogee Alta U9 cooled CCD camera with 3072(H)×2048(V) active pixels. X-ray images are taken every 1° around a 360° path during CT image acquisition and result in a local time-averaged phase distribution CT image. Since the liquid jet is issued into an air-filled environment, the CT images provide an outline of the gas-liquid interface.

Scans were conducted for this study with the camera system set for 4×4 binning and an exposure time of 1 second per projection. Binning is the adding together of signals from adjacent pixels, both horizontally and vertically, and is typically specified as the number of active horizontal pixels by the number of active vertical pixels. Binning is performed to decrease the image acquisition time and reduce the image file size. For example, a 2×2 binning and an exposure time of 2 seconds per projection were also completed but the file size exceeded 1 GB and file manipulation and data analysis become too cumbersome so these images were discarded. The X-ray source was operated at 4.5 mA and at 150 kV (higher voltages saturated the X-ray image and reduced the contrast at the gas-liquid interface). Two copper filters with thicknesses of 1 mm and one 1.55 mm-thick aluminum filter were used to reduce beam hardening effects [7], but a beam hardening correction algorithm was not applied to the data because it was not needed for the required analysis. Figure 2 shows the jet impingement flow loop mounted in the X-ray flow visualization facility.

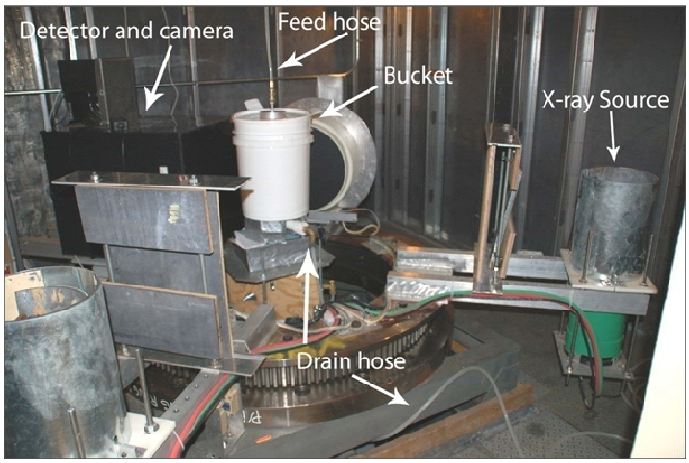

FIGURE 2: THE JET IMPINGEMENT FLOW LOOP LOCATED IN THE X-RAY FLOW VISUALIZATION FACILITY; THE PUMP AND MOTOR CONTROLLER ARE OUT OF THE IMAGE TO THE RIGHT.

The hydraulic jumps resulting from two different water flow rates (2.22 lpm and 2.75 lpm) were imaged in this study. A no-flow CT image was also acquired to provide a reference for the acrylic disk location and appearance. The Reynolds number of the jet flow at each flow rate, based on jet internal diameter and mean exit velocity, was 9700 and 12000, respectively. It should be noted that Reynolds numbers of these magnitudes for round pipe flow are generally considered turbulent, but Kate et al. [5] found that jet Reynolds numbers had to reach 26000 before the effects of turbulence appeared in the circular hydraulic jump.

The 360 X-ray projections for each test condition were reconstructed into 3D images using custom software developed by Iowa State University's Center for Nondestructive Evaluation. The depth of the liquid films before and after the jump and the radii of the hydraulic jump were then measured from these images.

RESULTS and DISCUSSION

Four CT scans of circular hydraulic jumps were analyzed: 2 trials with a water flow rate of 2.22 lpm (Re = 9700) and 2 trials at 2.75 lpm (Re = 12000). Figure 3a shows a picture of a hydraulic jump test in operation. For this picture, the nozzle assembly was raised to allow for visual access and photography. The water droplets are located on the underside of the acrylic disk while the water flows over the top of the disk in a smooth fashion. The location of the hydraulic jump is identified by the arrows. Figure 3b shows a single radiograph of the jet impingement process. Note that a radiograph is a 2D projection of a 3D process so the hydraulic jump is not apparent because the jump region is obscured by the fluid outside the jump region.

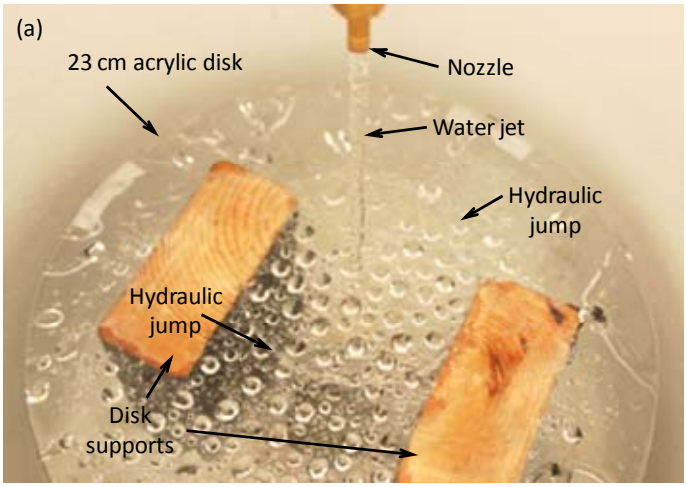

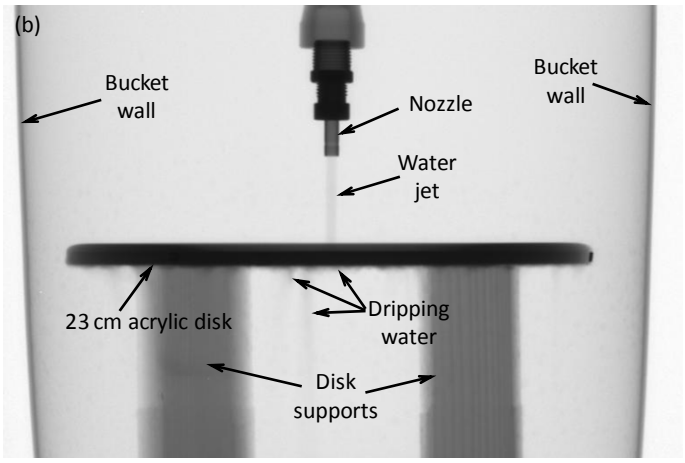

FIGURE 3: THE IMPINGING JET DURING OPERATION: (a) A VISIBLE LIGHT PICTURE OF THE BUCKET INTERIOR WHERE THE CIRCULAR HYDRAULIC JUMP CAN BE SEEN SURROUNDING THE JET, AND (b) A SINGLE RADIOGRAPH OF AN IDENTICAL PROCESS.

A single 3D reconstruction of the impinging jet and disk is shown in Figure 4 for Re = 12000. Similar results are observed when Re = 9700. The image shows the external extent of the nozzle and water region on a time-averaged basis. The hydraulic jump is identified by the dashed circular region. The "bumps" along the edges of the image show drop regions that were time-averaged.

The 3D CT image in Figure 4 can be "sliced" to show internal features and structures. Two such slices are shown in Figures 5 and 6. The vertical slice through the jet centerline is shown in Figure 5. The acrylic density is not too dissimilar to that of water so the CT intensity is similar between the acrylic and water regions. The color variation in the radial direction of the disk and water region is due to beam hardening effects [7]; the images in this study have not been corrected for this X-ray imaging phenomena because we are only interested in the gas-liquid interface to identify the hydraulic jump.

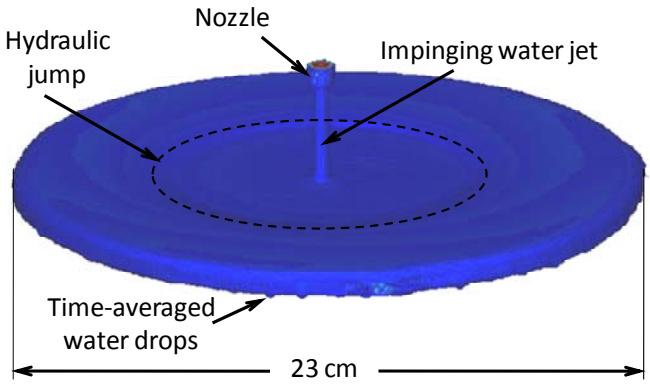

FIGURE 4: RECONSTRUCTED 3D CT IMAGE OF THE IMPINGING WATER JET AND HYDRAULIC JUMP FOR Re = 12000.

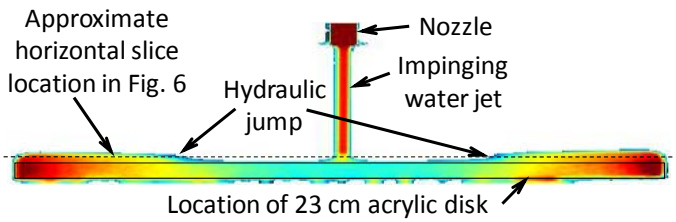

FIGURE 5: VERTICAL SLICE OF THE 3D RECONSTRUCTED CT IMAGE THROUGH THE JET CENTERLINE FOR Re = 12000.

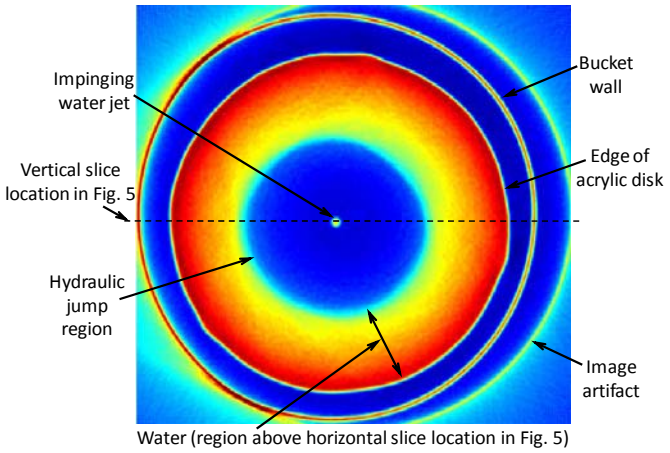

FIGURE 6: HORIZONTAL SLICE OF THE 3D RECONSTRUCTED CT IMAGE THROUGH THE HYDRAULIC JUMP REGION FOR Re = 12000.

The hydraulic jump region can be easily identified by slicing Figure 4 horizontally through the hydraulic jump region, as shown in Figure 6. The approximate location of this slice is identified in Figure 5. The fluid thickness before and after the hydraulic jump and the radial location of the hydraulic jump can be measured from the vertical and horizontal slices, respectively.

The average film thickness (h_1 and h_2 in Figure 1) for both flow rates were found to be $h_1 \approx 0.4$ mm and $h_2 \approx 3.6$ mm. It should be noted that the resolution of these images in the vertical direction was 0.4 mm/pixel, which limited the accuracy of the measurement of h_1. These values were compared to data from Rao and Arakeri [3]. While Rao and Arakeri's setup was not identical to the setup used in this paper, it was similar enough to allow some rough comparison. Indeed, their h_1 depth of approximately 0.3 mm was comparable to our results, but their h_2 value of approximately 1.6 mm was not. This discrepancy can likely be attributed to the difference in experimental equipment. Rao and Arakeri's particular set of data comparing radius and film thickness was recorded using an aluminum plate with a diameter of 30.6 cm. After examining other data recovered from experiments with this type of plate, it was found that, all other aspects of the experiment being equal, this type of plate produced much larger jump radii than smaller acrylic plates used by Rao and Arakeri. Although Rao and Arakeri did not report film thicknesses for these other plates, the jump radii were consistent with our results. This indicates that the aluminum plate likely provided less flow resistance than the acrylic plates, which allowed for larger jump radii and a corresponding smaller film thickness.

The value most thoroughly analyzed and compared with previous investigations is the radius of the circular hydraulic jump. Using horizontal slices of each scan, the radius was measured in three places: at the beginning and end of the jump region, and through the jump at a height halfway between h_1 and h_2. Figure 7 shows points on the radius at the half-height graphed around the jet impingement point, which was placed at the graph's origin. This was done to display the repeatability of the experiment and also to show that the hydraulic jumps produced were not always perfectly circular. This irregularity in radius could be attributed to several factors, the main ones being imperfections on the surface of the acrylic and/or interior of the nozzle and a slight non-normal impingement by the jet upon the acrylic surface. Depicted in Figure 7 with dashed lines are the average radii of the hydraulic jump as measured at the beginning and end of the jump region. Since the mid-height measurements are closer to the beginning of the jump region, one can conclude that the hydraulic jump undergoes an abrupt change in height and then it slowly levels off. As expected, the jump radius increases with Reynolds number .

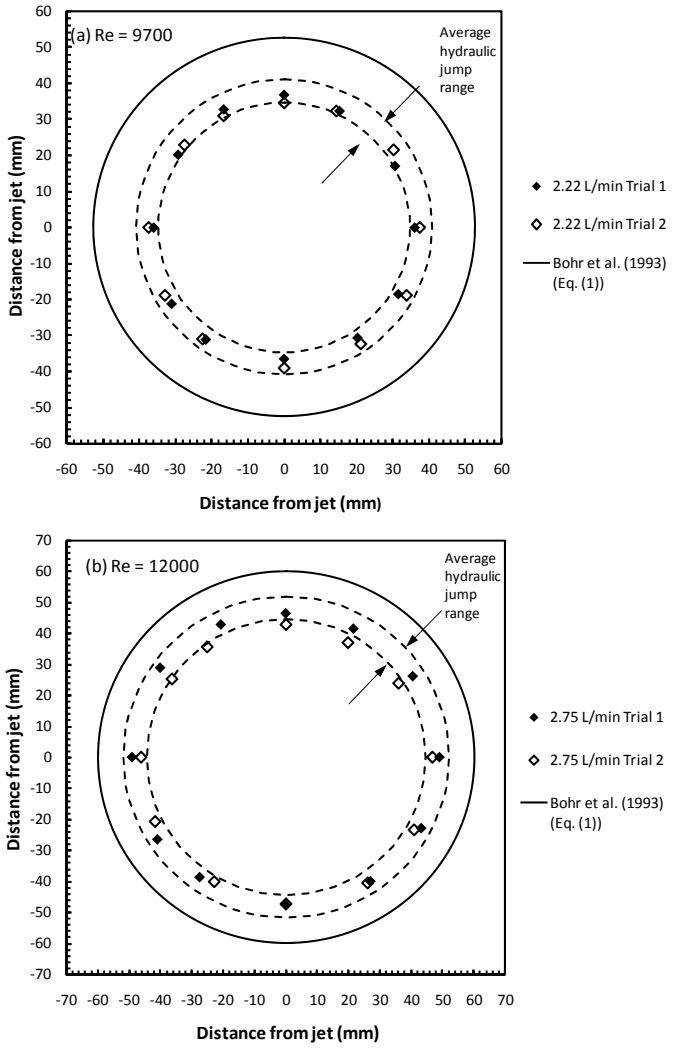

FIGURE 7: HYDRAULIC JUMP RADII AS MEASURED FROM THE CT IMAGES ON THREE DIFFERENT HORIZONTAL PLANES FOR (a) Re = 9700 AND (b) Re = 12000.

The solid line in Figure 7 shows the hydraulic jump radius as found through a scaling relation by Bohr et al. [8]:

$$R_j \approx \gamma = Cq^{5/8}\nu^{-3/8}g^{-1/8} \quad (1)$$

where R_j is the radius of the hydraulic jump, $q = Q/2\pi$ with Q the volumetric flow rate, ν is the kinematic viscosity, g is the acceleration due to gravity, and C is a constant whose value is based on the jet velocity profile. Since the jet flow is assumed to be laminar [5], the velocity profile was modeled as parabolic which corresponds to a value of $C \approx 0.73$ [8]. While the predicted value of R_j using Eq. (1) is larger than that determined experimentally, Figure 8 shows that our findings are quite similar to those of Rao and Arakeri [3] for a comparable setup. Note that the experimental values for the current study in Figure 8 show the average measurements taken at the hydraulic jump mid-height and the error bars represent the average radius at the beginning and end of the hydraulic jump. These ranges were included because most studies do not stipulate the location at which the hydraulic jump measurements are obtained.

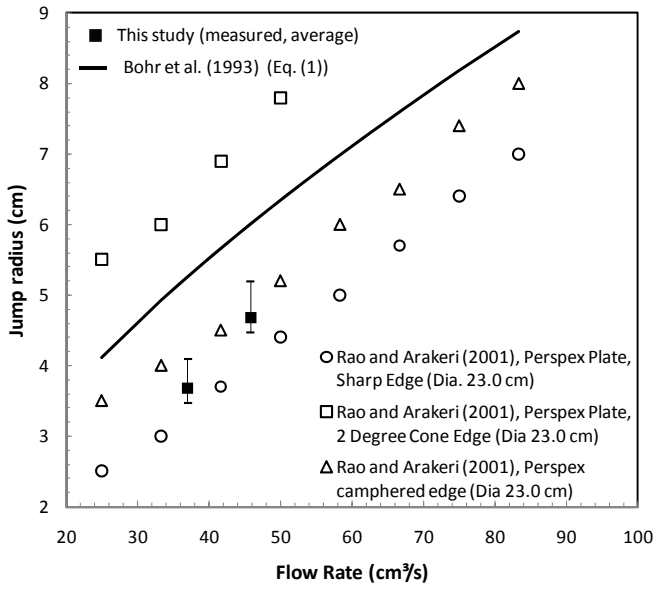

FIGURE 8: HYDRAULIC JUMP RADIUS AS A FUNCTION OF JET EXIT FLOW RATE COMPARED TO BOHR ET AL. [8] (EQ. (1)) AND SELECTED DATA FROM RAO AND ARAKERI [3]. THE BARS ON THE MEASURED DATA POINTS REPRESENT THE RANGE FROM THE BEGINNING TO THE END OF THE HYDRAULIC JUMP, WHEREAS THE DATA POINTS ARE THE AVERAGE OF THE HALF-HEIGHT MEASUREMENTS

CONCLUSIONS and RECOMMENDATIONS

The circular hydraulic jump was characterized in this study using X-ray computed tomography where a clear 3D image of the hydraulic jump was produced for analysis. These images allowed for measurement of both the hydraulic jump radius and depth with a single data acquisition method. The measurements obtained with this method were similar to those results available in the literature.

To improve the measurements, particularly in the film thickness before and after the hydraulic jump, higher spatial resolution CT imaging should be completed. For example, the scans analyzed in this study were performed at 4×4 binning, so it could be possible to obtain a finer resolution by using a smaller binning such as 2×2 or even 1×1. Unfortunately, these types of scans produce very large image files when trying to capture the entire hydraulic jump region, making analysis slow and cumbersome. This could be improved by focusing on only a small region in the jump region, but this too has challenges due to the potential to generate CT imaging artifacts when omitting regions during data acquisition. Nevertheless, a lower binning setting is required to better quantify the film thickness.

ACKNOWLEDGMENTS

MRD acknowledges the Iowa State University Program for Women in Science and Engineering Summer Internship Program for financial support. The X-ray facility used in this research was funded by the National Science Foundation under award number CTS-0216367 and Iowa State University.

REFERENCES

[1] Ellegaard, C., Hansen, A.E., Haaning, A., and Bohr, T., "Experimental Results on Flow Separation and Transitions in the Circular Hydraulic Jump," *Physica Scripta*, T67: 105-110 (1996).

[2] Naraghri, M.N., Moallemi, M.K., Naraghi, M.H.N., and Kumar, S., "Experimental Modeling of Circular Hydraulic Jump by the Impingement of a Water Column on a Horizontal Disk," *Journal of Fluids Engineering*, 121: 86-92 (1999).

[3] Rao, A. and Arakeri, J.H., "Wave Structure in the Radial Film Flow with a Circular Hydraulic Jump," *Experiments in Fluids*, 31: 542-549 (2001).

[4] Stevens, J.W., "Free Surface Flow Profile and Fluctuations of a Circular Hydraulic Jump Formed by an Impinging Jet," *Journal of Fluids Engineering*, 117: 677-682 (1995).

[5] Kate, R.P., Das, P.K., and Chakraborty, S., "Hydraulic Jumps Due to Oblique Impingement of Circular Liquid Jets on a Flat Horizontal Surface," *Journal of Fluid Mechanics*, 573: 247-263 (2007).

[6] Craik, A.D.D., Latham, R.C., Fawkes, M.J., and Gribbon, P.W.F., "The Circular Hydraulic Jump," *Journal of Fluid Mechanics*, 112: 347-362 (1981).

[7] Heindel, T.J., Gray, J.N., and Jensen, T.C., "An X-Ray System for Visualizing Fluid Flows," *Flow Measurement and Instrumentation*, 19(2): 67-78 (2008).

[8] Bohr, T., Dimon, P., and Putkaradze, V., "Shallow-Water Approach to the Circular Hydraulic Jump," *Journal of Fluid Mechanics*, 254: 635-648 (1993).